Histological and molecular characterization of the GAN diet-induced obese mouse model of advanced MASH with progression to advanced fibrosis and HCC

Authors
Monika Lewinska[1], Maja Andersen[1], Susanne Pors[1], Mogens Vyberg[2], Michael Feigh[1], Henrik H. Hansen[1]

[1]Gubra, Hørsholm Kongevej 11B, Hørsholm, Denmark
[2]Aalborg University, Center for RNA Medicine, Department of Clinical Medicine, Copenhagen, Denmark

Corresponding author
Monika Lewinska - **mle@gubra.dk**

Background & Aim

Metabolic dysfunction-associated steatohepatitis (MASH) is a leading cause of liver cirrhosis and hepatocellular carcinoma (MASH-HCC). However, the molecular alterations leading to onset of MASH-HCC are unclear. The present study aimed to evaluate disease progression in the translational GAN diet-induced obese (DIO) mouse model of advanced fibrosing MASH-HCC (GAN DIO-MASH-HCC mice).

Methods

Male C57BL/6J mice were fed the GAN diet high in saturated fat, fructose and cholesterol for 38-72 weeks (n=15 per group). Mice fed chow for 48-68 weeks (n=15) served as healthy controls. Terminal endpoints included AI-assisted Gubra Histopathological Objective Scoring Technique (GHOST) for NAFLD Activity Score and Fibrosis Stage and histomorphometrics, flow cytometry, tumor classification by an expert clinical histopathologist. Bulk RNA sequencing analysis was performed applying single sample gene set enrichment analysis (ssGSEA) and digital cytometry (xCell, EcoTyper). Transcriptional profiles of murine MASH and MASH-HCC were compared to hepatic transcriptomes from human MASH-HCC patients (n=45, GSE193084).

www.gubra.dk

1 Study outline and disease progression

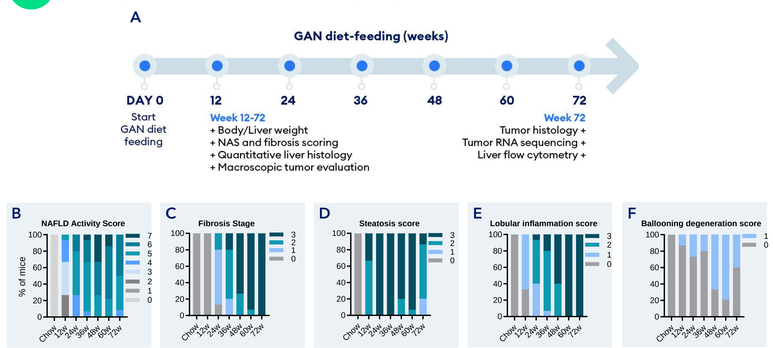

Figure 1. Disease progression in GAN DIO-MASH-HCC mice. GAN DIO-MASH-HCC mice show progressive development of severe NASH with advanced fibrosis. Mice were fed the GAN diet for 12–72 weeks (n = 15 per group). Chow-fed mice (n = 10) served as normal controls. **(A)** Study outline and endpoints. Histopathological scores were determined by deep learning-based image analysis using Gubra Histopathological Objective Scoring Technique (GHOST) for **(B)** NAFLD Activity Score (NAS), **(C)** Fibrosis stage, **(D)** Steatosis score, **(E)** Lobular inflammation score, and **(F)** Hepatocyte ballooning degeneration score.

2 Tumor occurrence

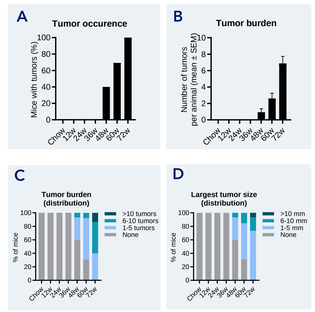

Figure 2. Tumor occurrence in GAN DIO-MASH-HCC model. GAN DIO-MASH-HCC mice show progressive HCC burden. Mice were fed the GAN diet for 12–72 weeks (n = 15 per group). Chow-fed mice (n = 10) served as normal controls. **(A)** Tumor occurrence. **(B)** Tumor burden. **(C)** Distribution of tumor burden in the cohort. **(D)** Distribution of largest tumor size in the cohort

3 Tumor histological classification

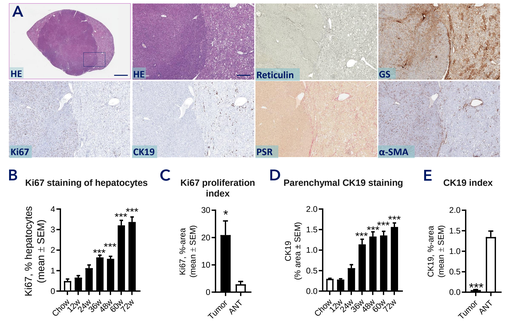

Figure 3. Histological characterization of tumors in GAN DIO-MASH. (A) Histological staining of liver neoplastic lesions in GAN DIO-MASH-HCC mice **(A)** Tumors were typically devoid of lipid droplets, extensive reticulin trabecular framework and diffuse glutamine synthetase staining, being histological characteristics of HCC. **(B)** Ki67 staining of hepatocytes (relative number, %; area, mm2). **(C)** Proportionate (%) area of Ki67 in tumor (n = 5 HCCs) vs. adjacent non-tumorous (ANT) liver tissue. **(D)** Proportionate (%) area of parenchymal CK19 staining. **(E)** CK19 staining in tumors (n = 5 HCCs) vs. adjacent non-tumorous (ANT) liver tissue. *p < 0.05, ***p < 0.001 versus surrounding tissue (t-test). Scale bar, 100 µm.

Conclusion

- The GAN-DIO-MASH-HCC mouse spontaneously develops HCC on the background of progressive advanced fibrosis
- HCC molecular signature in
- GAN DIO-MASH-HCC mice recapitulates poor prognostic human MASH-HCC and HCC immune microenvironment
- The translational GAN DIO-MASH-HCC mouse model is highly applicable for profiling novel drug therapies targeting NASH-HCC, including first-line immune checkpoint inhibitor therapies

Scan the QR code to see the poster online

4 Tumor molecular classification

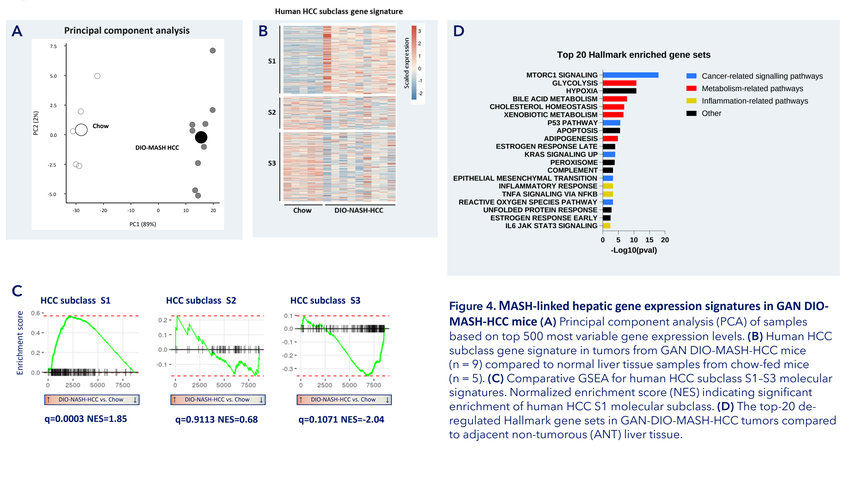

Figure 4. MASH-linked hepatic gene expression signatures in GAN DIO-MASH-HCC mice (A) Principal component analysis (PCA) of samples based on top 500 most variable gene expression levels. **(B)** Human HCC subclass gene signature in tumors from GAN DIO-MASH-HCC mice (n = 9) compared to normal liver tissue samples from chow-fed mice (n = 5). **(C)** Comparative GSEA for human HCC subclass S1–S3 molecular signatures. Normalized enrichment score (NES) indicating significant enrichment of human HCC S1 molecular subclass. **(D)** The top-20 de-regulated Hallmark gene sets in GAN-DIO-MASH-HCC tumors compared to adjacent non-tumorous (ANT) liver tissue.

5 Tumor immune microenvironment

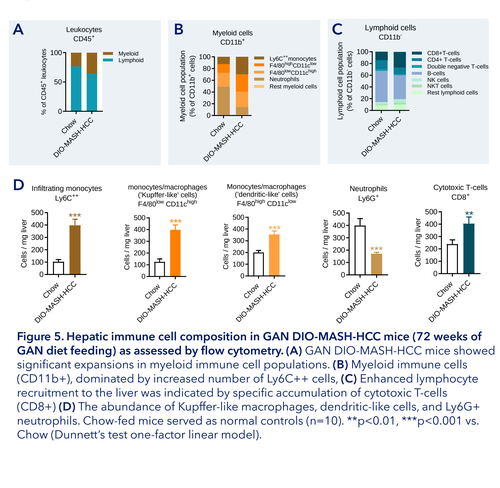

Figure 5. Hepatic immune cell composition in GAN DIO-MASH-HCC mice (72 weeks of GAN diet feeding) as assessed by flow cytometry. (A) GAN DIO-MASH-HCC mice showed significant expansions in myeloid immune cell populations. **(B)** Myeloid immune cells (CD11b+), dominated by increased number of Ly6C++ cells, **(C)** Enhanced lymphocyte recruitment to the liver was indicated by specific accumulation of cytotoxic T-cells (CD8+) **(D)** The abundance of Kupffer-like macrophages, dendritic-like cells, and Ly6G+ neutrophils. Chow-fed mice served as normal controls (n=10). **p<0.01, ***p<0.001 vs. Chow (Dunnett's test one-factor linear model).

6 Hepatic Immune Ecotype

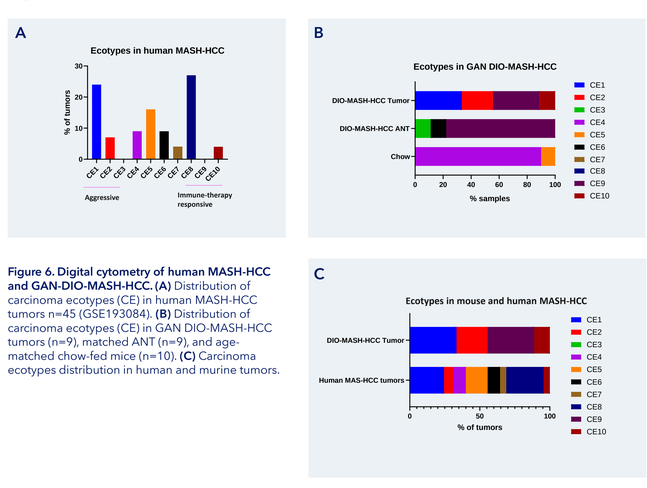

Figure 6. Digital cytometry of human MASH-HCC and GAN-DIO-MASH-HCC. (A) Distribution of carcinoma ecotypes (CE) in human MASH-HCC tumors n=45 (GSE193084). **(B)** Distribution of carcinoma ecotypes (CE) in GAN DIO-MASH-HCC tumors (n=9), matched ANT (n=9), and age-matched chow-fed mice (n=10). **(C)** Carcinoma ecotypes distribution in human and murine tumors.